



## Hardware Article

## An automated chemical vapor deposition setup for 2D materials

A.K. Niketa\*, Md Aasif Iqbal, Susmitha Kothapalli, Shishir Kumar

Department of Electrical Engineering, Indian Institute of Technology, Hyderabad, India



## ARTICLE INFO

## Article history:

Received 17 September 2020

Received in revised form 11 December 2020

Accepted 11 December 2020

## Keywords:

CVD

Automation

2D materials

## ABSTRACT

Chemical vapour deposition (CVD) provides a versatile and scalable route to synthesize various 2D materials. Lowering the barrier for access, customization, and cost of CVD equipment will benefit a large and multidisciplinary research community. We report an open-source and automated CVD setup which can be built incrementally to cover a large parameter space of CVD growth. Extensions are also discussed. The setup was validated by CVD graphene growth and characterization on Cu foils. The software controller forms a crucial part of the system. Its plug-in based approach for devices and abstraction of interactions as structured text, enables easy automation, extension, and accessibility. These features also allow the same controller core to be used for control of diverse laboratory equipment, of which we provide a couple of examples. Together, the hardware and software design provides an easy and versatile package for CVD setup, which can also be a starting point for several other automated instruments.

© 2020 Published by Elsevier Ltd. This is an open access article under the CC BY-NC-ND license (<http://creativecommons.org/licenses/by-nc-nd/4.0/>).

## 1. Introduction

## 1.1. Specifications table

Hardware name	AutoCVD
Subject area	Engineering and Material Science
Hardware type	Material synthesis using chemical vapour deposition
Open Source License	Hardware: CERN-OHLS v2 or later Software: GPL Documentation: CC BY
Cost of Hardware	\$26000
Source File Repository	<a href="https://doi.org/10.17605/OSF.IO/WU4JM">https://doi.org/10.17605/OSF.IO/WU4JM</a>

\* Corresponding author.

E-mail addresses: [ee19resch11010@iith.ac.in](mailto:ee19resch11010@iith.ac.in) (A.K. Niketa), [shishir@ee.iith.ac.in](mailto:shishir@ee.iith.ac.in) (S. Kumar).

## 2. Hardware in context

A large part of research on 2D materials is dependent on the availability of low cost, scalable methods to synthesize these materials to the desired quality and to introduce variations in them. CVD fills this role well and, therefore, has prominently commanded the attention of the researchers. As a result, many of the 2D materials, e.g., graphene [1], MoS<sub>2</sub> [2], BN [3], can be grown by CVD methods. CVD growth of 2D materials is generally done in a temperature and pressure-controlled vacuum chamber by flowing in the required gases to obtain a deposit on top of a substrate. The process is straightforward to scale and to control for the quality and composition of the deposit. Thus, CVD turns out to be a cost-effective, high throughput, and versatile synthesis method of 2D materials.

The CVD growth apparatus plays a critical role in this task, but its design has not been adequately addressed in the literature. Even though the literature has ample information about process development and optimization for the synthesis of 2D materials, we find limited details about the hardware and software used to implement that process. Recently, some articles have remedied the situation to some extent [4,5].

The high cost and closed source nature of the commercial equipment for CVD synthesis of 2D materials hamper their use in research laboratories. The wide variety of applications and experiments that are investigated with 2D materials require the CVD equipment to be customized and optimized for many cases. This is either not possible or is hard to accomplish with closed source hardware and software. Further, the design choices made with the commercial equipment require expertise which is not easily available within laboratories.

Here, we detail an open source, automated and extensible platform (AutoCVD) for CVD growth of 2D materials. The setup can control a wide range of gas flows and pressure, the two critical process parameters, which allows the implementation of broader sets of recipes available in the literature. A conscious choice has been made to use hardware, specially the electrical interfacing and computer control, which should be more familiar to the researchers.

The control software follows the same principles of extensibility and modularity. To provide these features, a plug-in architecture to integrate the hardware devices has been used. The core of the software manages the interaction between the clients and the individual devices in the setup. The functionality can be accessed transparently over a network by exchanging a series of command-response strings. This enables the scripting of the interaction. Scripts management tools are also included.

Two additional features of the software make it useful for a wider audience. First, it can be used to control a variety of experimental setups just by creating new plug-in devices. We provide a couple of such examples in the following sections. Second, the example interface for the CVD setup can be accessed by a browser, which is compactly described with the help of custom web components. Similar components can be built for any other system.

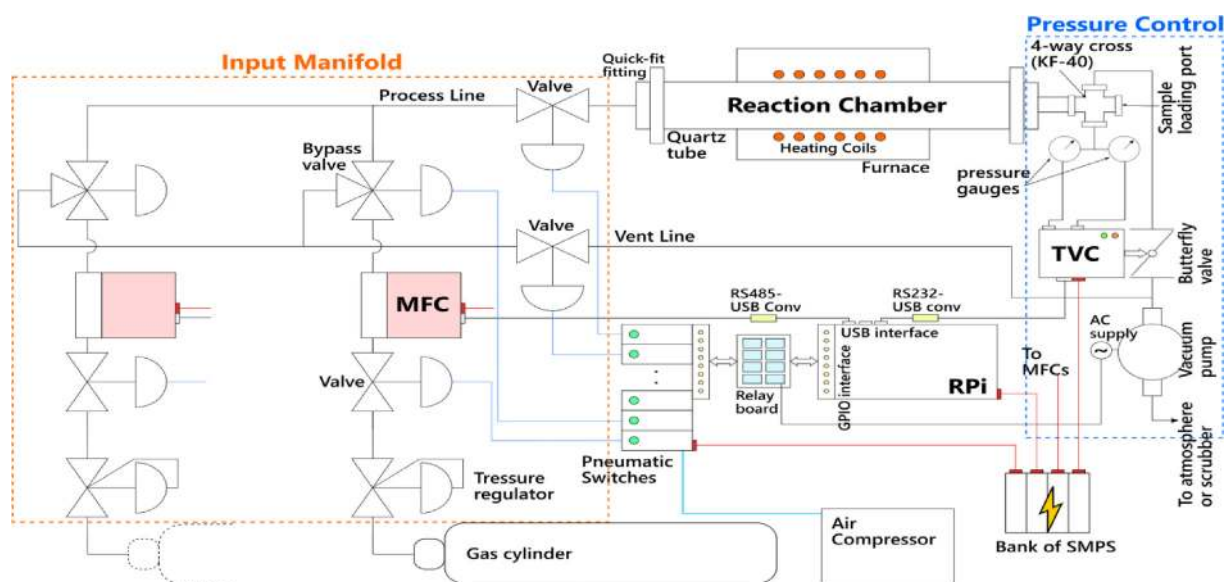


**Fig. 1.** Schematic of the system. The input manifold on the left-hand side feeds the process gases to the reaction chamber, whose outlet is connected to the pressure control unit consisting of a butterfly valve followed by a rotary pump.

### 3. Hardware description

The CVD setup as shown in Fig. 1 can be subdivided into hardware and software subsystems. Hardware subsystem consisted of a gas manifold, the reaction chamber, and a pressure monitor unit, while the software subsystem consisted of interface and control software. A single-board computer (SBC) hosted the software and interfaced with the hardware via its IO ports. Several switched-mode power supplies (SMPS) were used to power the components of the system. A detailed description follows.

#### 3.1. Hardware subsystem

The organization of the main components of the system is shown in Fig. 2. An inlet gas manifold feeds the desired gas mixture at a specific rate to the reaction chamber, whose pressure is controlled by a pressure control unit. The inlet gas manifold started at the gas cylinders. The cylinders, holding the process gases, were capped by stainless steel gas regulators and were housed in a ventilated gas cabinet beside the reactor. The outlet of a regulator was fed into a diaphragm valve, followed by a mass flow controller (MFC) and then, a bypass valve. Both the valves were pneumatically actuated. The diaphragm valve isolated MFCs from the gas cylinder when not activated. The bypass valve, in its default state, provided a path for process gas to merge in a common vent line, which was directly connected to the pump in the pressure control unit. Upon actuation, the bypass valves directed a process gas to the reaction chamber via a common inlet tube. The presence of bypass valves allows quick switching of gas flow to the chamber. They can be omitted in a simpler system. Both the main inlet tube and vent tube had one additional diaphragm valve to switch on and off the flow. Four gas lines were used on the inlet manifold -  $H_2$ ,  $CH_4$ ,  $N_2$ , and Ar. Blanked ports were left in the manifold for future expansion. The multi-gas multi-range (MGMR) digital MFCs were configured for the particular gas and the desired range. One just has to replace a cylinder and configure MGMR MFCs accordingly to use a different gas on an existing line. This allows a given system to be used for growth 2D materials from disparate sources.

The reaction chamber was a 1" quartz tube terminated by quick-fit vacuum fittings at the two ends. The middle section of the tube was located inside the heated portion of a resistive tube furnace. The furnace could go up to 1200C and had a PID controller for setting the temperature. Swagelok VCR compatible face seal fittings and 1/4" stainless steel tubings were used for connecting these items together. An alternative is to use Swagelok ferrule fittings, which are more accessible and cost-effective. These fittings do not need an orbital welder for the installation, thereby could be installed in most labs. However, their leak rates are higher than the face seal fittings, and should be evaluated for safety.

The input manifold can be modified in several ways - filters can be inserted in gas lines for purification, bubblers can be used to deliver volatile reactants, remote plasma generators can be attached for the supply of free radicals. Plasma generation can also be done by coupling electrodes directly on the quartz tube that forms the reaction chamber. The compressed air (C.A.) for pneumatic actuation of the valves was derived from an array of pneumatic switches. The input to this array was CA at 5–7 bars supplied by a compressor. The array was switched by electronic relays, which were controlled via the general-purpose Input Output (GPIO) lines on the single-board computer (SBC).

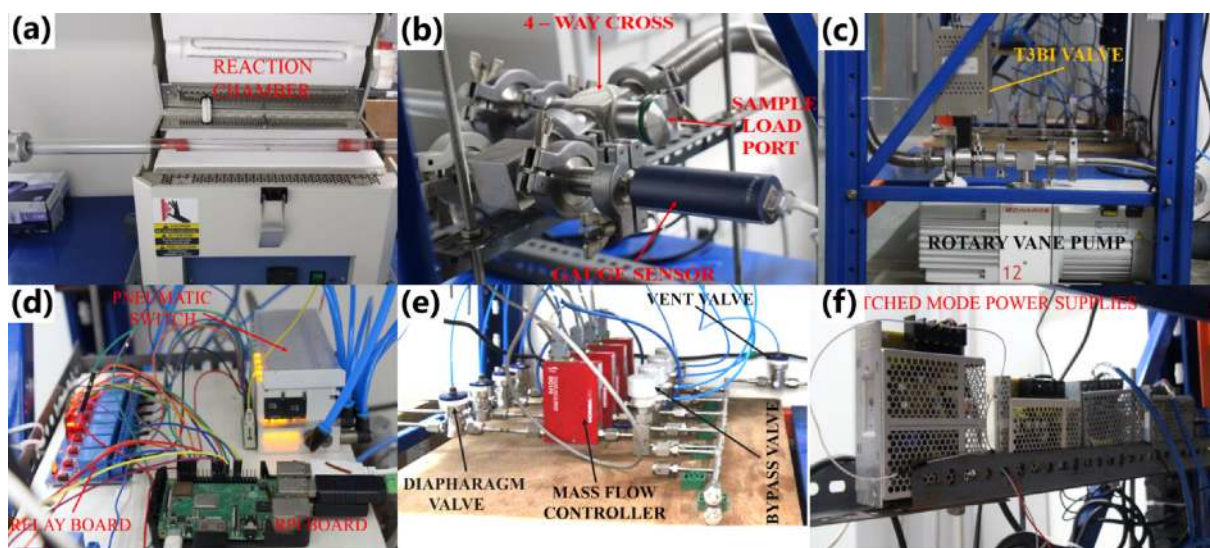


**Fig. 2.** Photographs of the various components of the system. (a) The reaction chamber: quartz tube inside a tube furnace, (b) the sample inlet port and gauges on KF-40 cross at the outlet of the reaction chamber, (c) the TVC (MKS T3Bi) and the pump, (d) the pneumatic and electronic relays and RPi3B board, (e) input manifold showing 4 sticks of process gases, each with two diaphragm valves and a mass flow controller and (f) the power supply units.

Downstream of the reaction chamber was attached to one of the ports of a KF-40 cross. Of the other three ports, one was meant for loading samples in the chamber. A long quartz rod was used to move samples from the loading port to the middle of the quartz tube. The KF-40 blank on the loading port was held in place by the vacuum inside the tube. It provided protection against overpressure. For atmospheric pressure CVD (APCVD) it can be held by a clamp. Another port of the KF-40 cross was connected to the throttle valve controller (TVC) and subsequently to the pump, using a flexible stainless steel hose. The specific TVC was chosen for its ability to probe two pressure gauges over their combined range. The last port of the cross was connected to two pressure gauges with ranges from 10 mtorr–10 torr and from 1 torr to 1000 torrs respectively. Together, they provided a total serviceable range of 5 decades. The overlap in their range was required for reliable switching of pressure by the TVC. The valve controller supplied power and control signals to the gauges. The valve was connected to the computer over a serial port and can be commanded to track the pressure or position of the valve. The throttle valve controller restricted the suction of process gas from the reaction chamber by the rotary vane pump, which was chosen to provide sub-10 mtorr pressure in the setup to the atmosphere.

These components were controlled and monitored by the Raspberry Pi 3B (Rpi) SBC. Several communication channels connected the SBC to respective digital interfaces on the devices. A two-wire RS485 channel was tapped off to connect all the MFCs. An RS485-USB converter provided a serial port on Rpi to communicate with the MFCs. The throttle valve presented an RS232 interface, which was converted to USB using an RS232-USB bridge. The electronic interface on the MFCs and throttle valve was chosen to be compatible with communication over the USB ports of Rpi. Other industrial interfaces can also be considered in the design, based on familiarity, access, and cost of the connectors and controllers.

A series of switched-mode power supplies (SMPS) was used to deliver D.C. voltages needed by electronics. The solid-state relay board worked on 5VDC and switched 24VDC lines based on logical control signals from the general-purpose Input Output (GPIO) of Rpi. The switched D.C. lines were connected to the pneumatic switches. One of the solid-state relays controlled the power supply to the rotary pump.

The system was hosted in a pallet racking system having three levels. An exhaust port was connected to the top level, the lowest was used for the gas manifold and electronics, whereas the reaction chamber sat on the middle rack. The pallet rack can be covered with hard plastic sheets from the sides for isolation. A gas abatement system should be used in line with the exhaust port when dealing with toxic gases.

### 3.2. Software subsystem

The control software core consisted of a controller with which new devices could be registered at the time when the core starts. The devices to be registered were listed in a configuration file which the core read. The configuration information consisted of device identifiers, their default parameters, and communication channel specifications. The core then probed the device drivers for exposed functionality and then, for initialization of devices and communication channels. Once the initialization was over, the core listened to a network port as a network server, waiting to act as a conduit between clients and the devices.

Upon a successful network connection with the controller server, the clients sent command(s) for the devices to perform operations. The controller parsed this text request and invoked appropriate functionality from the drivers. The response returned by the drivers was packed and sent to the appropriate client by the controller. In the same manner, the controller's functionality itself was also dynamically changed, e.g., to enable logging, to save and load-scripts. The use of formatted request-response enabled scripting of process control. The format for request-response was expressed in JavaScript Object Notation (JSON) and consisted of a list of data items. For the requests, the list had device identifiers, commands, and any arguments in that order. For the responses, the list had the status followed by the response returned from the device. Multiple clients can be active simultaneously. A simple access control mechanism was also included to handle conflicts that may arise in shared network access.

An HTTP server wrapped the network interface into a WebSocket interface to enable browser-based clients. We developed an HTML based graphical user interface (GUI) for the system, which can be accessed from any modern browser. A notable feature of the GUI was the use of Web components specification for generating custom HTML elements, representing the devices attached to the system. Custom elements provided a compact, reusable, and modular representation of the devices. Fig. 3 Shows this GUI in action. The HTML GUI ran a javascript loop to monitor and display all the relevant parameters of the system. User interaction in the form of mouse or keyboard input generated asynchronous javascript events that were relayed to the controller, if appropriate. Subsequently, the display was updated when a response was received. All the commands generated from user interactions were recorded with a timestamp in the GUI itself and could be saved as scripts. Later, these scripts were used for automated sessions.

## 4. Discussion

The flow controllers used are multi-gas and multi-range (MG-MR) digital MFCs. These MFCs can be configured by software to be used for a specific gas in one of the three non-overlapping ranges. The total span of ranges can be chosen while ordering and remains fixed after that. The MFCs allow for any of the gas sources to be used by only changing the gas cylinders. For example, to vary the carbon source, one gas from a bank of methane, ethene and acetylene can be selectively routed

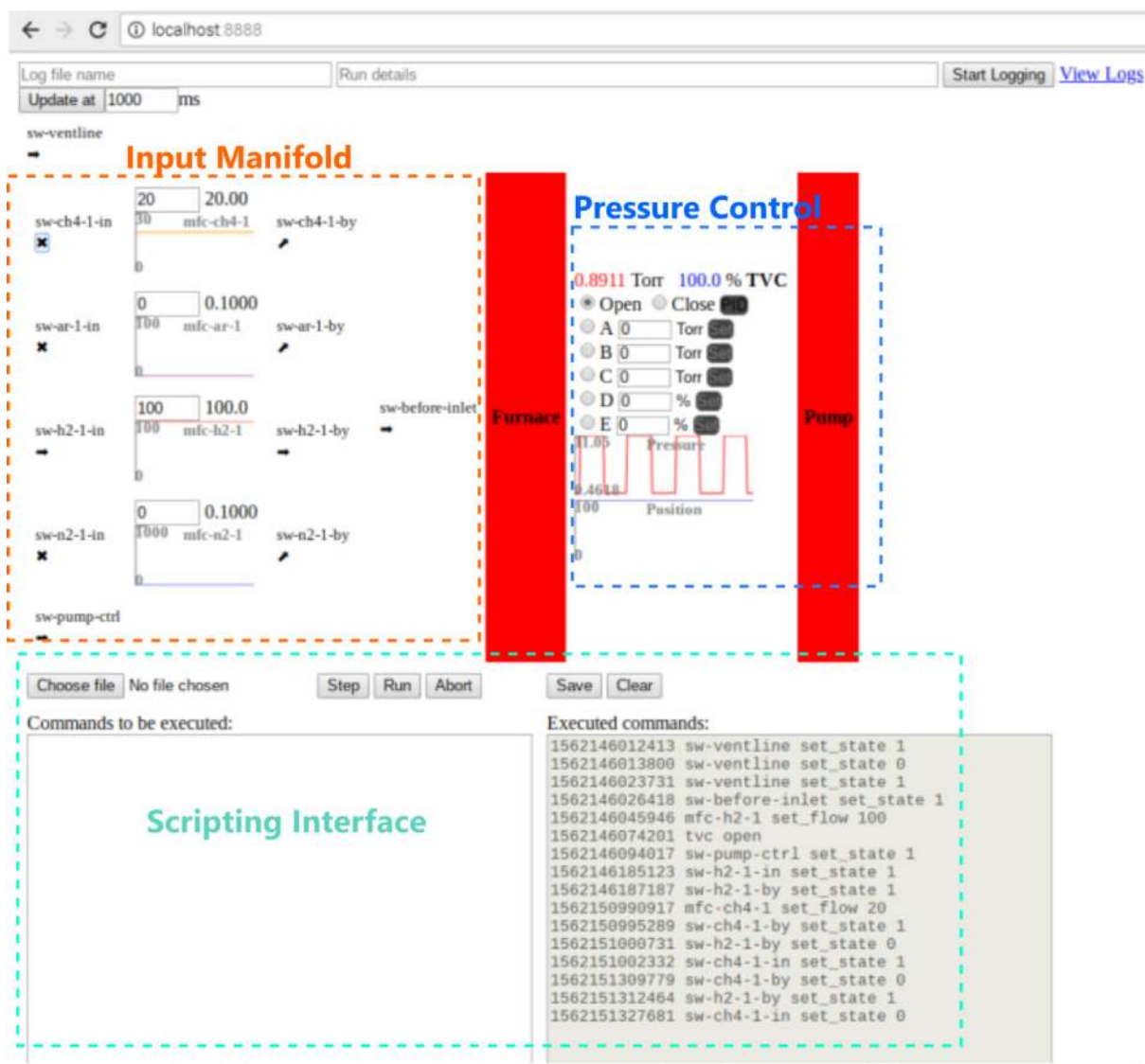


Fig. 3. GUI screenshot of the system showing the elements corresponding to the input manifold, pressure control unit and the scripting interface.

to a properly configured MG-MR MFC using diaphragm valves. More importantly, the variable range of the MFCs allow access to 3 times wider range of gas flows compared to normal MFCs. This is especially important for tuning the ratio of hydrogen and carbon precursor and the flow rate of methane. Ratios ranging from 1000 to less than 1 and minute methane flows have been used previously [6]. In our setup, the methane MFC has ranges of three non-overlapping ranges spanning 3–31 sccm, whereas the hydrogen MFC can range from 200 sccm to 800 sccm. With these values, it is easy to go for minute flow of methane as well as tuning the  $\text{H}_2:\text{CH}_4$  ratio as desired. Other benefits of digital MFCs include higher functionality, immunity to noise and easier integration.

Besides using the MG-MR MFCs, the input manifold had ports available for expansion. Such expansion may be needed for adding volatile gases, e.g. ammonia. The input manifold also allows external access to the quartz tube of the reaction chamber, which makes it possible to install electrodes for plasma generation or heaters for volatile substances, e.g. sulphur.

The pressure control unit of the system was driven by a TVC, which could probe two pressure gauges. In our setup, the gauges span 10 mtorr to 10 torr and 1 torr to 1000 torr ranges respectively, giving a coverage of 5 decades. Thus, the recipes demanding very low pressure growth to atmospheric growths can be run in this setup. The TVC provides other advanced functionality for optimizing the process, like control over response time, crossover points and backfill routines. For even more exact control over the system, the gauges can be read by the single board computer (SBC) and throttle valve controller can be commanded accordingly. This requires the SBC to have analog inputs or digital ports, which is the case here.

The software control system was designed for enforcing repeatability and reducing the variability in setting the process parameters. All the commands executed by the system and the response to them are recorded with millisecond resolution timestamps. The millisecond resolution is better than the response time of any of the devices on the system. Since the commands and responses are text based, it is easy to review them for process tracing and to edit recipes. Recipes are also straightforward to write from scratch. The recipes can also be executed in “dry-run” mode, where the selected device drivers respond with dummy data. The selection can be made in the configuration file. This is quite useful to check the sequence of execution without flowing gases. These facilities, combined together, allow reduction of human error and effort and improve access by new or infrequent users.

The control software was specifically architected to serve as a controller for a wide range of systems. A software controller is a recurring need in research laboratories and may also be helpful in industrial settings. To the best of our knowledge, there is no open source software to address this requirement. In most cases reported in literature, a custom controller is written, often in Labview, to interact with the instruments. It is hard to repurpose such work for a completely different system because they tightly couple the functionality for instrument interaction, control operations and user interaction. The controller software presented here, maintains the separation of functionalities of devices and interfaces, making it repurpose. The reuse of code also brings additional benefits of lower cognitive load on users and developers, as well as lower incidence of bugs.

To achieve this modularity, we have standardized a text interface for the interactions between clients and the devices. It allows the interpretation of the commands and responses to be embedded in the device drivers or the user interface. Then, the controller core is only responsible for facilitating the interaction between the clients and the devices. The device drivers appear as plug-ins to the core, exposing only as much functionality from the device as is needed. The drivers can also be developed independently from the core and therefore, are portable across different systems. Similarly, the user interfaces can be customized independently. The use of open source and widely used languages - Python for the core and device drivers and Javascript for the user interface - allows wider accessibility.

## 5. Design files

### 5.1. Design files summary

## 6. Bill of materials

The approximate cost associated with each item used to build the CVD setup is shown in the table below. Many of the items were procured from local vendors as indicated (see [Table 2](#)).

## 7. Build instructions

Detailed build instructions for the connections between components is detailed in the design file listed in [Table 1](#). Here we provide the instructions for the overall system only.

### 7.1. Input gas manifold

The input gas manifold can be built in-house or can be fabricated from external vendors. For in-house built, access to an orbital welder is necessary if the face seal fittings are used. The steps for assembling the gas manifold are:

1. Order the main components (valves, MFCs) compatible with the specifications needed. This step requires that the design of gas manifold and electrical connections is available in detail, so that the appropriate electrical and vacuum port endings can be selected.
2. Determine the number, lengths and type of vacuum fittings (e.g. face seal assemblies, tees, crosses, SS tubing, welding points) that will be used. Similarly determine the pneumatic fittings (tubings, tees and crosses) requirements from the design. Electrical cabling and connectors need to be specified at this stage.
3. Weld the tubing and fittings as required by the design.
4. Assemble the vacuum fittings on an appropriate support, say a metal plate.
5. Make electrical and pneumatic connections for the components.

**Table 1**  
Design files and their location.

Design file name	File type	Open source license	Location of the file
hardware-connections.odt	OpenDocument Text	CC BY	<a href="https://doi.org/10.17605/OSF.IO/WU4JM">https://doi.org/10.17605/OSF.IO/WU4JM</a>
BoQ-CVD-furnace.ods	OpenDocument Spreadsheet	CC BY	<a href="https://doi.org/10.17605/OSF.IO/WU4JM">https://doi.org/10.17605/OSF.IO/WU4JM</a>

**Table 2**  
Bill of quantities for the furnace.

Item	Vendor	Quantity	Total Price (\$), approximately
Bluetherm Split Furnace	Lindeberg	1	5000
Bypass Valve	Swagelok	4	4000
MFC N112	Horiba	4	4000
T3Bi Throttle Valve Controller	MKS	1	4000
Diaphragm Valve (Normally Closed)	Swagelok	6	1800
RV11 Pump	Edwards Vacuum	1	1500
CDG020D pressure gauges	Inficon	2	1500
Pressure Regulator	Rotarex	4	1200
1/4" SS tubing	Valex	30 m	300
Pneumatic Switch Array	Festo	1 (24 switches)	300
Pallet Rack	Local	1	300
Gas Cylinders	Local	4	200
Quick-Fit Connectors 1"	Local	2	200
Compressor	Local	1	200
SMPS (+-15 V, 0-24 V, 0-5 V)	Omron	4	150
Relay Boards	Unknown	3 (8 + 8 + 4 relays)	100
Quartz Tube 1"	Local	1	100
KF40 Cross	Local	1	100
Pneumatic fittings	Local	1	100
Raspberry Pi 3B	CarzyPi.com	1	50
4 mm Nylon tubing	Local	10 m	50
RS485-USB converter	Local	1	20
RS232-USB converter	Local	1	10
Electrical Wiring	Local	10 m	20
Enclosure sheets	Local	1	50
		Total	25,250

## 7.2. Pressure control unit

The pressure control unit integrates the gauges, the throttle valve controller and the pump using KF fittings. The fittings should be purchased matching to the ports available on these devices. Once all the fittings are available, they can be connected as shown in Fig. 4.

## 7.3. Electrical and electronic components

The power supply and control connections needed to operate the input gas manifold, the reaction chamber and the pressure control unit are listed in the design file (Table 1).

## 7.4. Enclosure and scaffold

The reaction chamber is a quartz tube, which needs mechanical support in the form of a scaffold. In our setup, the support was made of slotted angle bars, which allowed for change in scaffold height and length, to accommodate various quartz tubes.

The enclosure was a pallet rack, which was assembled in the laboratory using the instructions provided by the vendor.

## 8. Operation instructions

### 8.1. Safety Considerations:

#### 8.1.1. Exhaust and ventilation

The growth process of 2D materials often uses toxic or inflammable gases. As mentioned earlier, the leakages should be contained by use of properly evacuated gas cabinets as well as the reactor enclosure. The toxic gases in the exhaust can be fed through a gas abatement system before release into the atmosphere. The work areas should be properly ventilated at all times to reduce the chances of accumulation of gases. Gas detectors can also be installed and coupled with the control system to shut down the system in case of leaks. Leak checks should be done at periodic intervals as a part of maintenance of the system. Scripted control of the system minimizes the incidences of human errors and at the same time provides opportunities for automated testing of the system (e.g. for leaks).

#### 8.1.2. Furnace operation

The furnace should be monitored for proper operation, especially when it is heating.

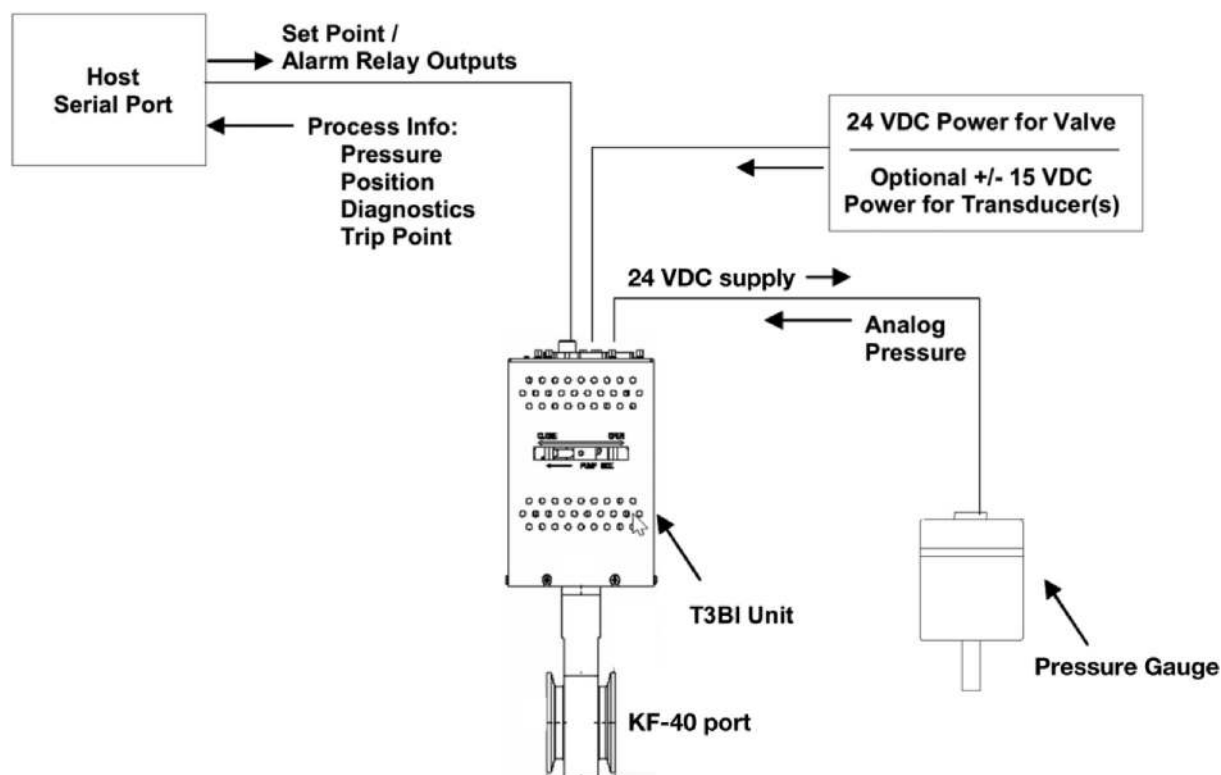


**Fig. 4.** Connection diagram of the pressure control unit. The KF-40 ports on the TVC (T3Bi) are connected to the pump and the reaction chamber. Only one of the two pressure gauges is shown.

## 8.2. Software Operation:

1. Turn on the power supply to the compressor, the furnace and the SMPS bank in that order.
2. After the computer boots up, open a terminal and run the interface server (e.g. `python3 interfaceserver.py`). It starts the control server in the background. The control server should display the initialisation information of all the devices that were listed in the configuration file.
3. Now open a browser and go to <http://localhost:8888> to access the GUI interface.
4. Turn on the gas regulators to supply the gases to the input manifold.
5. Operate the CVD setup as needed by the growth recipe, either manually or by the scripting interface.
6. Turn off the gas regulators.
7. After the growth process is finished, the browser can be closed and the interface server process can be killed.
8. Power down the computer, the SMPS bank, the furnace and the compressor in that order.

## 9. Validation and characterization

Automated CVD described here is used for graphene growth. For sizable single-layer graphene copper as a substrate is used. A piece of copper foil was cleaned with acetone followed by isopropyl alcohol and then blow-dried. The cleaned foil was slid in the reaction chamber using a long quartz rod. The chamber was then evacuated by the rotary vane pump to a pressure of <math><100\text{ mTorr}</math>. The furnace was ramped to  $1000\text{ }^{\circ}\text{C}$  in 30 mins under a flow of  $100\text{ sccm H}_2$  at a pressure of about 1 Torr. The foil was annealed at  $1000\text{ }^{\circ}\text{C}$  for 1 h under  $100\text{ sccm}$  of  $\text{H}_2$  to reduce the surface defect density and to increase the Cu grain size. Under the same conditions, methane was added to flow at  $2\text{ SCCM}$  for 20 min. The furnace was shut off to cool down the reaction chamber in the gas flow of  $100\text{ sccm}$  of  $\text{H}_2$ . The Cu foil was taken out from the tube at room temperature (Fig. 5).

CVD growth of graphene on Cu foils is well established in literature [7]. The particular recipe that we have used results in low density of graphene nucleation sites [8], therefore, large final polycrystals. SEM images can quickly tell about the coverage of graphene on the sample. For the sample shown in Fig. 5, we see multiple graphene crystals,  $20\text{ }\mu\text{m}$  in size, growing nearby. They also appear to be single-layered, which was further supported by the Raman spectrum obtained from the sample. The size of crystals is close to what was expected from the growth recipe. Raman spectrum of ideal graphene crystal



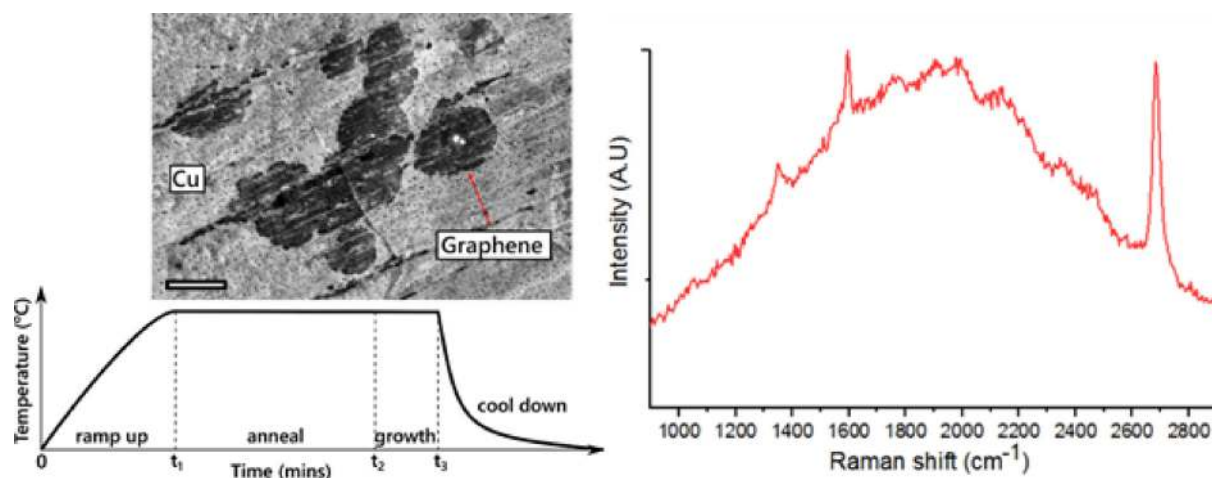


**Fig. 5.** The plot shows the CVD growth process used here, consisting of ramp-up, annealing, growth, and cool-down phases. See text for process gases,  $t_1$ ,  $t_2$ , and  $t_3$ . SEM image shows the isolated graphene deposits lying on Cu foil (scale bar is 20  $\mu\text{m}$ ). Raman spectrum indicates single layer graphene with some defects.

consists of a G-peak, located at  $\sim 1580 \text{ cm}^{-1}$  and a 2D peak located at  $\sim 2685 \text{ cm}^{-1}$ . For single layer graphene, the ratio of the latter to the former is 3–4 and the full width half maximum of the latter is  $\sim 30 \text{ cm}^{-1}$ . Defects show up as the D peak at  $\sim 1350 \text{ cm}^{-1}$ . With increasing disorder, the ratio of D to G peaks and the width of these peaks increases, whereas the 2D peak disappears. The sample shown in Fig. 5 has a pronounced broad background, which typically appears due to the Cu substrate on which graphene is grown. The sharp 2D and G peaks and the relative strength of these peaks indicate good quality single layer graphene. The Raman signal also sampled the edges of the crystals, since their size is small as seen in the SEM images. This is indicated by a small D peak seen in the spectrum.

Here, we have shown only one set of growth parameters that leads to graphene growth. Large numbers of recipes have been reported in the literature [7] for tuning the growth leading to graphene having particular properties. The choice of hardware components made on the system allows for exploration of a large subset of these recipes.

## 10. Conclusion

We have successfully designed and programmed an open source CVD system that enables growth of graphene layers on the Cu foil. Optimised system design incorporating inlet gas manifold, reaction chamber, pressure control unit with an efficient software including GUI interface realise the automated system with reduced cost as compared to the existing commercial CVD systems. Additionally, due to the expandable architecture of facilitating new plug in devices, modifications can be applied and customised accordingly. This design paves way for research in nanomaterials with lower startup cost leading to advancement in the arena of 2D materials.

## CRediT authorship contribution statement

**A.K. Niketa:** Validation. **Md Aasif Ikbal:** Software, Validation. **Shishir Kumar:** Conceptualization, Methodology, Software, Resources, Supervision.

## Declaration of Competing Interest

The authors declare that they have no known competing financial interests or personal relationships that could have appeared to influence the work reported in this paper

## Acknowledgements

We would like to thank Ms. Ekta Prajapati for help in editing the manuscript.

## Funding

The equipment was funded by the department of Electrical Engineering, Indian Institute of Technology, Hyderabad. An earlier version of the equipment was funded by the Center for Nanoscience and Engineering (CeNSE) at Indian Institute of Science.

## Appendix A. Supplementary data

Supplementary data to this article can be found online at <https://doi.org/10.1016/j.ohx.2020.e00165>.

## References

- [1] X. Li et al, Large-area synthesis of high-quality and uniform graphene films on copper foils, *Science* 324 (2009) 1312–1314. <https://science.sciencemag.org/content/324/5932/1312>.
- [2] H. Schmidt et al, Transport properties of monolayer MoS<sub>2</sub> grown by chemical vapor deposition, *Nano Lett.* 14 (2014) 1909–1913. <https://pubs.acs.org/doi/10.1021/nl4046922>.
- [3] K.K. Kim, A. Hsu, X. Jia, S.M. Kim, Y. Shi, M. Hofmann, D. Nezich, J.F. Rodriguez-Nieva, M. Dresselhaus, T. Palacios, J. Kong, Synthesis of monolayer hexagonal boron nitride on Cu foil using chemical vapor deposition, *Nano Lett.* 12 (1) (2012) 161–166.
- [4] L.W. Godwin et al, Open-source automated chemical vapor deposition system for the production of two- dimensional nanomaterials, *PLOS ONE* 14 (2019), <https://doi.org/10.1371/journal.pone.0210817>.
- [5] J.H. Ahn, M. Na, S. Koo, H. Chun, I. Kim, J.W. Hur, J.H. Lee, J.G. Ok, Development of a fully automated desktop chemical vapor deposition system for programmable and controlled carbon nanotube growth, *Micro and Nano Syst Lett* 7 (1) (2019), <https://doi.org/10.1186/s40486-019-0091-8>.
- [6] I. Vlassiouk, M. Regmi, P. Fulvio, S. Dai, P. Datskos, G. Eres, S. Smirnov, Role of hydrogen in chemical vapor deposition growth of large single-crystal graphene, *ACS Nano* 5 (7) (2011) 6069–6076.
- [7] H.C. Lee, W.-W. Liu, S.-P. Chai, A.R. Mohamed, A. Aziz, C.-S. Khe, N.M.S. Hidayah, U. Hashim, Review of the synthesis, transfer, characterization and growth mechanisms of single and multilayer graphene, *RSC Adv.* 7 (26) (2017) 15644–15693, <https://doi.org/10.1039/C7RA00392G>.
- [8] P. Ghosh, S. Kumar, G. Ramalingam, V. Kochat, M. Radhakrishnan, S. Dhar, S. Suwas, A. Ghosh, N. Ravishankar, S. Raghavan, Insights on defect-mediated heterogeneous nucleation of graphene on copper, *J. Phys. Chem. C* 119 (5) (2015) 2513–2522, <https://doi.org/10.1021/jp510556t>.